Strangeness and Statistical QCD

Johann Rafelski[a*] and Jean Letessier[b†]

[a]Department of Physics, University of Arizona, Tucson, AZ 85721
and
CERN-Theory Division, 1211 Geneva 23, Switzerland

[b] Laboratoire de Physique Théorique et Hautes Energies
Université Paris 7, 2 place Jussieu, F–75251 Cedex 05.

We discuss properties of statistical QCD relevant in Fermi phase space model analysis of strange hadron production experimental data. We argue that the analysis results interpreted using established statistical QCD properties are demonstrating formation of the color deconfined state of matter in relativistic heavy ion collisions at highest CERN-SPS energies and at BNL-RHIC, comprising deconfined matter composed of nearly massless quarks and gluons, in statistical equilibrium.

1. INTRODUCTION

More than 20 years ago, several theoretical meetings held at the University Bielefeld have laid the foundation for the rapid analytical (perturbative QCD) and numerical (lattice QCD) development of Statistical Quantum Chromodynamics. We will illustrate in this paper, using as an example the strangeness signature of quark-gluon (color) plasma (QGP), the relevance of this work in the analysis of experimental data, and the resulting identification of quark-gluon plasma formation in relativistic heavy ion collisions.

The discovery of QGP, unlike the discovery of a new particle, requires a change in the understanding of fundamental hadronic degrees of freedom. The signature of QGP is very hard to identify, since the final state observed in the laboratory always consists of the same particles, irrespective of the transitional presence of the deconfined state. What changes is the detailed composition of the observed produced particle abundance. We consider here the disappearance of strangeness suppression, accompanied by a changed pattern of (enhanced) strange antibaryon production, with reestablished baryon-antibaryon symmetry of thermal spectra. All these phenomena offer compelling evidence for quark-gluon plasma formation [1–9].

To demonstrate the formation of QGP, we determine the physical properties of the source of hadronic particles we are observing, which we associate with the properties of statistical QCD. We show that the anomalous yields of strange hadrons originate from a state of matter with physical properties of a quark-gluon fireball. We begin with a short

*Supported by grant DE-FG03-95ER40937 from the U.S. Department of Energy.
†LPTHE, Univ. Paris 6 et 7 is: Unité mixte de Recherche du CNRS, UMR7589.

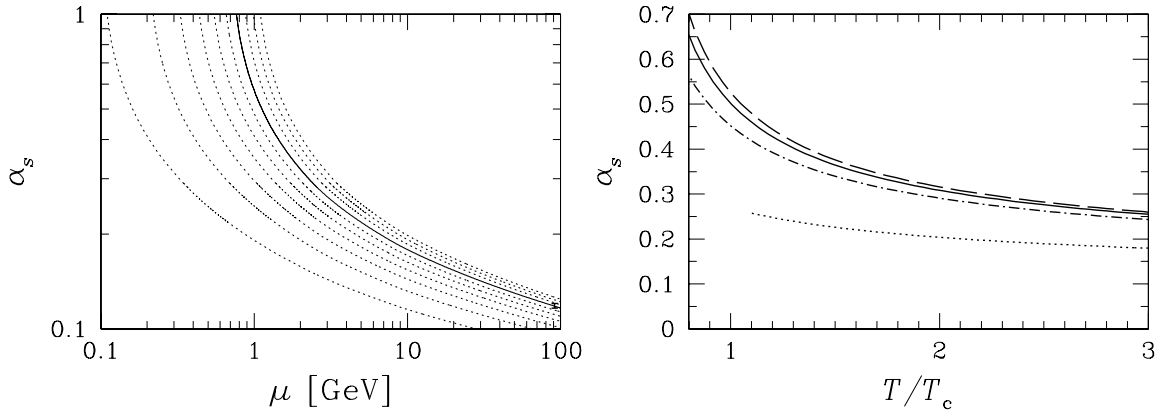

Figure 1. Left: $\alpha_s^{(4)}(\mu)$ as function of energy scale μ for a variety of initial conditions. Solid line: $\alpha_s(M_Z) = 0.1182$ (see the experimental point, which includes the error bar at $\mu = M_Z$; dotted lines: sensitivity to variation of the initial condition.
Right: $\alpha_s(2\pi T)$ for $T_c = 0.160\,\mathrm{GeV}$. Dashed line: $\alpha_s(M_Z) = 0.119$; solid line = 0.1181; dot-dashed line = 0.1156. Dotted line: approximate 2-loop solution, given in Eq. 1, with choice $\Lambda = 150$ MeV.

survey of statistical QCD results we employ, and follow this with a summary of results on hadron production and their interpretation in terms of the QGP state.

2. STATISTICAL QCD

2.1. Running coupling constant of QCD

For the purpose of quark–gluon plasma studies, we require the strength of QCD interaction, and the magnitude of quark mass as function of energy scale. The simplest way to obtain these results is to integrate the first order renormalization group equations using the perturbative definition of the β, γ functions, given an initial value of $\alpha_s(M)$ and $m_i(M)$. For the determination of the coupling constant, it has become common to refer to the value of $\alpha_s(M_Z = 91.19\,\mathrm{GeV})$. We use as the central value $\alpha_s(M_Z) = 0.1182 \pm 0.002$.

To obtain the solid line in figure Fig. 1 (left) the four-loop β-function was used, in the $\overline{MS}$ modified minimum subtraction scheme. The dotted lines demonstrate considerable sensitivity to the initial value $\alpha_s(M_Z)$. If $\alpha_s(M_Z)$ were larger, the evaluation of the coupling strength in the 'low' energy domain $\mu \lesssim 1$ GeV, of interest in QGP studies, would be divergent, see dotted lines in Fig. 1 (left) above the solid line. The criticism of the perturbative study of strangeness production derives from the belief that the strength of the QCD interaction is larger than is now known: to put it differently, an essential prerequirement for the perturbative theory of strangeness production in QGP, is the relatively small experimental value $\alpha_s(M_Z) \simeq 0.118$, which has been experimentally established in recent years. It is interesting to note in figure Fig. 1 (left) that a 20% reduction in $\alpha_s(M_Z)$ leads to a 'good' $\alpha_s(0.1\,\mathrm{GeV}) < 1$.

When studying thermal processes in QGP at temperature T, the proposed interaction scale is $\mu \equiv 2\pi T \simeq 1\,\mathrm{GeV}\ T/T_c$, for $T_c \simeq 160\,\mathrm{MeV}$. In Fig. 1 (right), the solid line corresponds to an exactly computed α_s with physical quark thresholds, evaluated at the thermal scale, and expressed in terms of T/T_c. The range of experimental uncertainty

in $\alpha_s(T)$, due to uncertainty in $\alpha_s(M_Z)$, is delimited by dashed and dot-dashed lines bordering the solid line. A popular approximation of α_s,

$$\overline{\alpha}_s^{(2)}(\mu) \simeq \frac{2}{b_0 \bar{L}} \left[1 - \frac{2b_1}{b_0^2} \frac{\ln \bar{L}}{\bar{L}} \right] , \quad \bar{L} \equiv \ln(\mu^2/\Lambda^2) \, , \tag{1}$$

agrees, using the standard value $\Lambda^{(5)} = 205 \pm 25$ MeV with exact solution for $\mu > 2m_b$. Presence of lighter quark loops leads to a major deviation at scales of interest to us. Eq. (1) is represented in Fig. 1 (right) by the dotted line, it misses the exact result by factor 2 for $T_{\rm c} < T < 1.75 T_{\rm c}$, the effective range of observables emerging in SPS and RHIC experiments. The experimental error in determination of α_s is today considerably smaller.

The high sensitivity of physical observables to α_s, which depend on $\alpha_s^n, n \geq 2$, makes it imperative that we do not rely on this approximation (dotted line in Fig. 1 (right)). Yet a fixed value $\alpha_s = 0.25$ (instead of $\alpha_s = 0.5$) derived from this approximation is still often used in a study of the QGP phase properties, energy loss of parton jets, charmed quark thermalization, strange quark thermal production, etc. Such treatment of QCD interaction underestimates by as much as factor four the interaction with the QGP phase, and thus the speed of these processes. In most cases, this mundane factor matters, and we see that accurate evaluation of α_s at the appropriate physical scale is required.

2.2. Quark–gluon plasma pressure and phase boundary

The partition function (i.e., pressure) of the quark–gluon phase is obtained after we combine quarks, gluons and vacuum contributions:

$$\frac{T}{V} \ln \mathcal{Z}_{\rm QGP} \equiv P_{\rm QGP} = -\mathcal{B} + \frac{8}{45\pi^2} c_1 (\pi T)^4 + \frac{n_{\rm f}}{15\pi^2} \left[\frac{7}{4} c_2 (\pi T)^4 + \frac{15}{2} c_3 \left(\mu_{\rm q}^2 (\pi T)^2 + \frac{1}{2} \mu_{\rm q}^4 \right) \right] . \tag{2}$$

We have inserted here the appropriate quark ($n_{\rm f} = 2$) and gluon degeneracy. The interactions between quarks and gluons manifest their presence aside of the vacuum structure effect $\mathcal{B}$, in the three coefficients $c_i \neq 1$, see [10]:

$$c_1 = 1 - \frac{15\alpha_s}{4\pi} + \cdots , \quad c_2 = 1 - \frac{50\alpha_s}{21\pi} + \cdots , \quad c_3 = 1 - \frac{2\alpha_s}{\pi} + \cdots . \tag{3}$$

While higher order terms in the perturbative expansion have been obtained, they suggest lack of convergence of the expansion scheme formulated today. Given that the lowest order terms are consistent with thermal lattice results we do not pursue this issue further. Rather, we show for which parameter set the lattice and perturbative statistical QCD results agree with each other and we use these results to understand the properties of a QGP fireball. To reproduce the lattice results, near to $T = T_{\rm c}$, the only choice we can make is in value of the bag constant, $\mathcal{B} = 0.19\,{\rm GeV/fm}^3$.

Dotted lines in Fig. 2 show the QGP phase pressure condition $P_{\rm QGP} \to 0$ for different velocities of expansion, employing an extrapolation to finite baryochemical potential [11]. The solid line denotes, in the $\mu_{\rm b}$–T plane the pressure balance between an hadronic point particle gas and a stationary quark–gluon phase. Dashed line shows the phase boundary with an hadronic gas made of finite size hadrons. However, the fluid flow motion of quarks and gluons expands the domain of deconfinement exercising against the vacuum force originating in the collective expansion velocity $\vec{v}_{\rm c}$ [12].

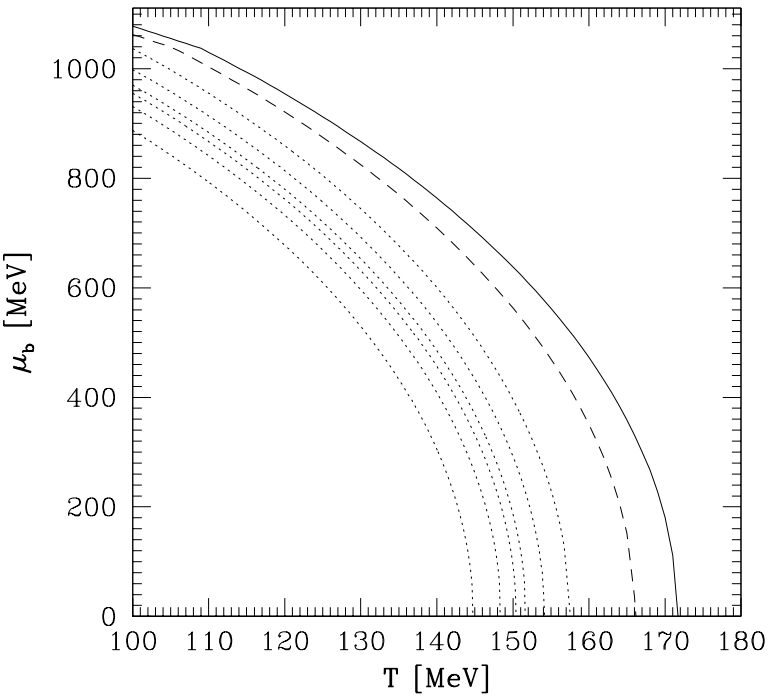

Figure 2. Pressure balance in $\mu_{\rm b}$–$T_{\rm c}$-plane. Dotted(from right to left): $P = 0$ at expansion velocity $v^2 = 0, 1/10, 1/6, 1/5, 1/4$ and $1/3$. Solid line, the phase boundary between hadron gas and QGP, with point hadrons, dashed the phase boundary with finite size hadrons.

The condition $P = P_{\rm p} - \mathcal{B} = 0$, including the effect of motion reads [13],

$$\mathcal{B} = P_{\rm p} + (P_{\rm p} + \epsilon_{\rm p})\frac{\kappa v_{\rm c}^2}{1 - v_{\rm c}^2}\,, \qquad \kappa = \frac{(\vec{v}_{\rm c} \cdot \vec{n})^2}{v_{\rm c}^2}\,, \tag{4}$$

where subscript p refers to particle pressure and energy, and where we introduced the geometric factor κ which characterizes the angular relation between the surface normal vector and flow direction.

Expansion beyond $P \to 0$ is in general not possible. A fireball surface region which reaches condition Eq. (4) and continues to flow outwards must be torn apart. This is a collective instability and the ensuing disintegration of the fireball matter should be very rapid. Thus we find, that a rapidly evolving fireball which supercools into the domain of negative pressure is in general highly unstable, and we expect that a sudden transformation (hadronization) into confined matter can ensue in such a condition. It is important to note that the situation we described could only arise since the vacuum pressure term is not subject to flow and always keeps the same value. Looking at the high flow velocity curves in Fig. 2 we see that an exploding QGP fireball only contained by the vacuum can supercool to $T \simeq 145$ MeV.

2.3. Thermal mass and QGP properties

It has been shown that it is also possible to reproduce the lattice results using fine tuned thermal masses (see table I in [14]). In Fig. 3, we show the light quark (solid thick line) and gluon (dashed thick line) thermal masses which were fitted to the lattice QGP

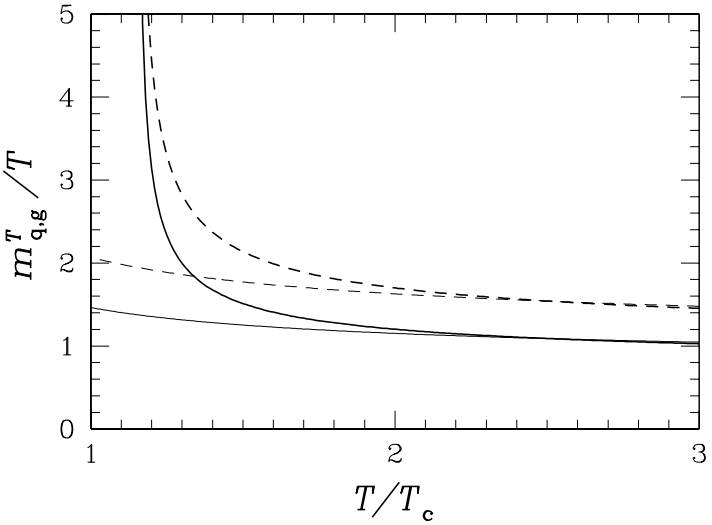

Figure 3. Thermal masses fitted to reproduce Lattice-QCD results [14], thick solid line for quarks, and thick dashed line for gluons. Thin lines, perturbative QCD masses for $\alpha_s(\mu = 2\pi T)$.

data. The perturbative thermal masses, definitions slightly modified compared to [15,16], are for quarks and gluons,

$$(m_{\rm q}^{\rm T})^2 = \frac{4\pi}{3}\alpha_s T^2\,, \qquad (m_{\rm g}^{\rm T})^2 = 2\pi\alpha_s T^2\left(1+\frac{n_{\rm f}}{6}\right)\,, \tag{5}$$

and are also shown in Fig. 3, thin lines (dashed for gluons) obtained using $\alpha_s(\mu = 2\pi T)$, see Fig. 1 (right).

We conclude that the thermal masses required to describe the reduction of the number of degrees of freedom for $T > 2T_{\rm c}$ are just the perturbative QCD result. Importantly, this means that thermal masses express, in a different way, the effect of perturbative QCD, and thus for $T > 2T_{\rm c}$, we have the option to use Eq. (2), or the more complex thermal mass approach.

The discussion of the properties of QGP is a wide subject which is beyond the scope of this report, and we conclude showing the entropy density as function of temperature in Fig. 4. The solid line is for the case of equilibrated quark-light glue system, in the limit of vanishing chemical potential. We note that initially the entropy rises faster than the asymptotic T^3 behavior, since the QCD interactions weaken, and there is an increase in the effective number of acting quark and gluon degrees of freedom. Thus, the drop in entropy density is considerable when plasma cools and approaches hadronization condition. In order to preserve the entropy content in the fireball when the system expands, from $T \simeq 300$ MeV towards 150 MeV, a volume dilution by a factor nine must occur. The 'pure glue' case (short-dashed line) contains as expected about half of the entropy when comparing at equal temperature, the addition of strangeness adds at the level of 10% to the entropy content, at a given temperature. However, as strangeness is produced temperature of the isolated fireball cools, and thus there entropy production is even smaller.

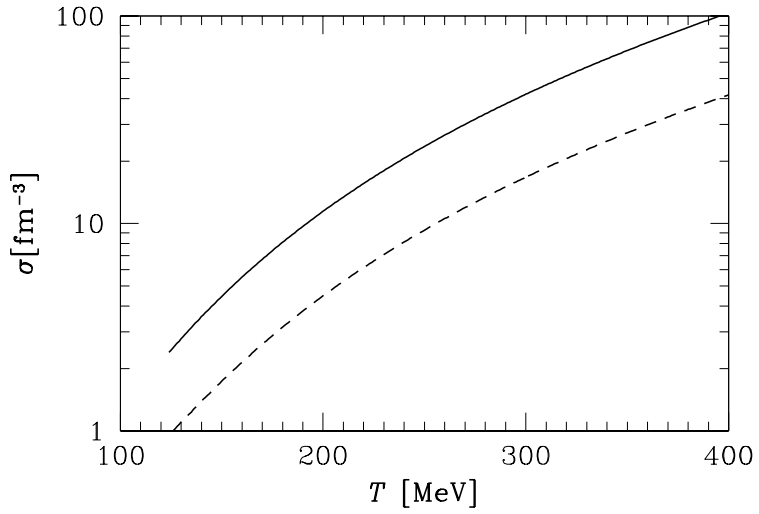

Figure 4. Entropy density in chemically equilibrated QGP at $\lambda_{\rm q} = 1$ as function of temperature. Solid line $n_{\rm f} = 2$, long dashed line $n_{\rm f} = 2.5$, short dashed line 'pure glue' $n_{\rm f} = 0$.

3. STRANGENESS PRODUCTION IN COLLISION PROCESSES

3.1. Remarks about thermal strangeness production

Strangeness, and more generally heavy flavor quarks, can be produced either in the first interactions of colliding matter, or in the many ensuing less energetic collisions. Strange quark mass $m_{\rm s}$ is comparable in magnitude to the typical temperatures reached in heavy ion interactions, and the numerous 'soft' secondary parton collisions dominate the production of strangeness, and naturally, of the light u, d flavors.

At the time strange flavor approaches chemical equilibrium in soft collisions, the back reaction is also relevant. The quantum mechanical matrix element driving a two-body reaction must be, channel by channel, the same for forward and backward going reactions due to time reversal symmetry. The actual rate of reaction differs, since there are usually considerable differences in statistical and phase space factors. However, the forward an backward reactions will balance when equilibrium particle yields are established. This principle of detailed balance can sometimes be used to evaluate one of the two reactions.

This is not the place to repeat the well known details of the kinetic theory of strangeness production, [8] based on the perturbative cross sections [17], evaluated with running QCD parameters, [18]. However, we note that the use of scale dependent QCD parameters, α_s and $m_{\rm s}$, with $\mu \propto \sqrt{s}$ amounts to a re-summation of many QCD diagrams comprising vertex, and self energy corrections. A remaining shortcoming of thermal production evaluation is that up to day, there has not been a study of the next to leading order final state accompanying gluon emission in thermal processes, e.g., $\mathrm{gg} \to \mathrm{s\bar{s}} + \mathrm{g}$. In direct parton induced reactions, this next to leading order effect enhances the production rate by a factor $K = 1.5$–3. This may cause a corresponding increase also in the thermal rate of production, and thus a reduction in the thermally computed chemical equilibration time of strangeness and charm. The magnitudes (up to 0.4 mb) of both types of reactions considered, quark fusion and gluon fusion, are similar. Gluons dominate flavor production, because they are so much more likely to collide in the appropriate production channel.

Given the cross section and collision frequency, the relaxation constant τ_s of chemical equilibration can be evaluated and the result is that it takes less than 2 fm/c to equilibrate strangeness if $T > 300$ MeV, and somewhat less time, in the event that next to leading order effects play an important role. Despite this clear indication of near strangeness equilibration in SPS and RHIC environment, there is considerable difference in the computational results [19–22], originating in differing assumptions about degree of chemical equilibration of gluons in the early stage of the QGP formation. The relaxation time is 4 times larger should gluons be only 50% equilibrated.

3.2. Strangeness background

One could argue that if strangeness is to be used as a diagnostic tool of quark–gluon plasma, we need to understand this background production rate of strange hadrons. In that context, we are interested to measure how often, compared to light quark pairs, strange quarks are made.

Wróblewski proposed to consider the strangeness suppression factor [23]:

$$W_s = \frac{2\langle s\bar{s}\rangle}{\langle u\bar{u}\rangle + \langle d\bar{d}\rangle}\,. \tag{6}$$

Only newly made $s\bar{s}$, $u\bar{u}$ and $d\bar{d}$ quark pairs are counted. If strangeness were to be as easily produced as light u, d quarks, we would find $W_s \to 1$. To obtain the experimental value for W_s, a careful study of produced hadron yields is required. We cite below results obtained using a semi-theoretical method [24], in which numerous particle yields are described within the framework of a statistical model. In elementary collisions pp, $p\bar{p}$, e^+e^-, a value $W_s \simeq 0.22$ is obtained, strangeness is thus relatively strongly suppressed. On the other hand, in nuclear A–A' collisions W_s more than doubles compared to p–p interactions, considered at the same energy.

To explain the 2–2.5-fold strangeness yield increase in a kinetic model of particle production requires a shift towards strangeness production of all particle formation processes. In other words, when modeling the enhanced strangeness yields within a variety of approaches, in each model a new reaction mechanism must be introduced that favors strangeness over none-strange processes. Even at this relatively elementary level of counting hadron abundances, new physics must be introduced. In a model with the deconfined phase this new reaction mechanism is due to the presence of mobile gluons, which are most effective in making strange quark pairs. Moreover, as the conditions created in the QGP become more extreme with collision energy, e.g., initial temperature exceeding substantially the strange quark mass, we expect an increase in W_s.

Generally hadron cascade models tuned to produce enough singly strange hadrons, predict wrong abundances of the rarely produced particles such as $\overline{\Xi}$, $\overline{\Omega}$. We are not aware of any kinetic hadron model with or without 'new physics' that is capable to reproduce the pattern of rare hadron production, along with enhancement of strangeness and hadron multiplicity. Moreover, if rapidity spectra are modeled, usually the transverse momentum spectra are incorrect, or vice-versa. It thus seems impossible, in a collision model based on confined hadron interactions, to find sufficiently many hadron–hadron collisions to occupy by hadrons the large phase space (high $p_\perp$, high y) filled by products of nuclear collision. If indeed a non-QGP reaction picture exists to explain heavy ion collision data, the current

situation suggests that some essential reaction mechanism has been overlooked for 20 years. In short, hadron models need a lot more effort to reach satisfactory agreement with the experimental results, even regarding rather simple observable such as hadron multiplicities, transverse energy production, strangeness yield. Strangeness production in thermal processes in hadronic gas were studied carefully [25,6], and the time scales involved established. It is impossible to explain the observed pattern of strange hadron production in kinetic thermal model based on confined hadron interactions.

Some researchers abandon the kinetic, i.e., collisional theory of particle production, and focus solely on the experimental fact that the observed hadronic multiplicities are result of a pre-established statistical distribution near to thermal and chemical equilibrium, which works quite well. However, it was already pointed out 15 years ago that such a result can be naturally explained in terms of a dynamic theory of a transient deconfined state hadronizing in a coalescence model [7]. A detailed study of the subtle deviations in hadron yields from precise statistical equilibrium yields allows to understand the hadronization mechanism [26], and therefore ultimately also to explore the properties of the hadronizing QGP state.

4. HADRON FREEZE-OUT

4.1. Chemical nonequilibrium in hadronization

An extra reaction step 'hadronization' is required to connect the properties of the deconfined quark–gluon matter fireball, and the experimental apparatus. In this process, the quark and gluon content of the fireball is transferred into ultimately free flowing hadronic particles. In hadronization, gluons fragment into quarks, and quarks coalesce into hadrons. Color 'freezes', quark–gluon plasma excess entropy has to find a way to get away, so any additional production is hindered. It is far from obvious that hadron phase space (so called 'hadronic gas') be used consistently to describe the physics of thermal hadronization, and we establish now the consistency criterion assuming that entropy production is small, or even null, in hadronization of entropy rich thermal QGP into entropy poor hadron phases space.

We consider the Gibbs–Duham relation for a unit volume, $\epsilon + P = T\sigma + \mu\nu$, and combine it with the instability condition of dynamical expansion, Eq. (4):

$$0 = P|_{\rm h} + (P|_{\rm h} + \epsilon|_{\rm h})\frac{\kappa v_{\rm c}^2}{1-v_{\rm c}^2}\,, \quad \left.\frac{\epsilon}{\sigma}\right|_{\rm h} = \left(T|_{\rm h} + \left.\frac{\mu_{\rm b}\nu_{\rm b}}{\sigma}\right|_{\rm h}\right)\left(1+\frac{\kappa v_{\rm c}^2}{1-v_{\rm c}^2}\right)\,. \tag{7}$$

Using global variables we obtain [13]:

$$\left.\frac{E}{S}\right|_{\rm h} = (T|_{\rm h} + \delta T|_{\rm h})\left(1+\frac{\kappa v_{\rm c}^2}{1-v_{\rm c}^2}\right)\,, \quad \delta T = \mu_{\rm b}\frac{\nu_{\rm b}}{\sigma} = \frac{\mu_{\rm b}}{S/b}\,. \tag{8}$$

For RHIC, we have $\delta T|_{\rm h} < 0.4$ MeV, considering that $\mu_{\rm b} < 40$ MeV and $S/b > 100$; at top SPS energy, we have $\mu_{\rm b} \simeq 200$–250 MeV and $S/b \simeq 25$–45, and thus, $\delta T|_{\rm h} \simeq 5$ MeV.

The particular usefulness of Eq. (8) comes from the observation that it implies:

$$\left.\frac{E}{S}\right|_{\rm h} > T|_{\rm h}\,. \tag{9}$$

This is a near equality since the geometric emissivity factor κ is positive and small, especially so at RHIC, and $v_c^2 < 1/3$.

The Gibbs–Duham relation implies: $E/S + PV/S = T + \delta T > T$. One would think that the PV term is small, since the pressure is small as the lattice calculations suggest, $\epsilon/P \to 7$. However, this effect can be compensated by large volume of hadronization. The volume is a directly measured quantity. The HBT results place a very severe constraint on the emitter size of the pion source. Another way, to constraint the magnitude of V, is to relate it to the total yield of pions. With these constraints, the PV term is negligible. In Eq. (8), due to super cooling, P was negative, and contributed the κ term on the right hand side.

Neglecting the influence of PV, we obtain just as in Eq. (9): $E/S \simeq T$. In Eq. (9), we have a universal hadronization constraint, which should be satisfied in models claiming to describe hadron production in relativistic heavy ion collisions. This constraint is, in our experience, difficult if not impossible to satisfy in chemical equilibrium statistical hadronization models. The reason is that, in such an approach, a rather high temperature $T \simeq 175$ MeV is required to accommodate the high intrinsic entropy content of hadron source, but this does not drive up sufficiently the energy content, since for pions in equilibrium $E/S < T$. In the super saturated ($\gamma_q \sim 1.6$) pion gas $E/S > T$.

4.2. Phase space and parameters

Our approach is in its spirit a generalization of Fermi's statistical model of hadron production [27,28], in that the yield of hadrons is solely dictated by the study of the magnitude of the phase space available.

The relative number of final state hadronic particles freezing out from, e.g., a thermal quark–gluon source, is obtained noting that the fugacity f_i of the i-th emitted composite hadronic particle containing k-components is derived from fugacities λ_k and phase space occupancies γ_k:

$$N_i \propto e^{-E_i/T_f} f_i = e^{-E_i/T_f} \prod_{k\in i} \gamma_k \lambda_k. \tag{10}$$

In most cases, we study chemical properties of light quarks u, d jointly, though on occasion, we will introduce the isospin asymmetry. As seen in Eq. (10), we study particle production in terms of five statistical parameters $T, \lambda_q, \lambda_s, \gamma_q, \gamma_s$. In addition, to describe the shape of spectra, one needs matter flow velocity parameters, these become irrelevant when only total particle abundances are studied, obtained integrating all of phase space, or equivalently in presence of strong longitudinal flow, when we are looking at a yield per unit of rapidity.

Assuming a QGP source, several of the statistical parameters have natural values:

1. λ_s: The value of strange quark fugacity λ_s can be obtained from the requirement that strangeness balances, $\langle n_s - n_{\bar{s}} \rangle = 0$, which for a source in which all $s, \bar{s}$ quarks are unbound and have symmetric phase space, implies $\lambda_s = 1$. However, the Coulomb distortion of the strange quark phase space plays an important role in the understanding of this constraint for Pb–Pb collisions, leading to the Coulomb-deformed value $\lambda_s \simeq 1.1$.

2. $\gamma_{\rm s}$: The strange quark phase space occupancy $\gamma_{\rm s}$ can be computed within the framework of kinetic theory and $\gamma_{\rm s} \simeq 1$. Recall that the the difference between the two different types of chemical parameters λ_i and γ_i is that the phase space occupancy factor γ_i regulates the number of pairs of flavor 'i', and hence applies in the same manner to particles and antiparticles, while fugacity λ_i applies only to particles, while λ_i^{-1} is the antiparticle fugacity.

3. $\lambda_{\rm q}$: The light quark fugacity $\lambda_{\rm q}$, or equivalently, the baryochemical potential $\mu_{\rm b}$, regulate the baryon density of the fireball and hadron freeze out. This density can vary dependent on the energy and size of colliding nuclei, and the value of $\lambda_{\rm q}$ is not easily predicted. However, it turns out that this is the most precisely measurable parameter, with everybody obtaining the same model independent answer, for it directly enters all very abundant hadrons. Since T differs depending on strategy of the analysis, the value of $\mu_{\rm b}$ is not so well determined and we recommend that $\lambda_{\rm q}$ be cited instead of $\mu_{\rm b} = 3T \ln \lambda_{\rm q}$.

4. $\gamma_{\rm q}$: The equilibrium phase space occupancy of light quarks $\gamma_{\rm q}$ is expected to significantly exceed unity to accommodate the excess entropy content in the plasma phase, $\gamma_{\rm q} \leq \gamma_{\rm q}^{\rm c} = e^{m_\pi/2T_{\rm f}} \simeq 1.6$.

5. $T_{\rm f}$: The freeze-out temperature $T_{\rm f}$ is expected to be within 10% of the Hagedorn temperature $T_H \simeq 160\,{\rm MeV}$, which characterized particle production in proton-proton reactions.

6. Turning now to the flow parameters: The collective expansion velocity $v_{\rm c}$ is expected to remain near to the relativistic sound velocity, $v_{\rm c} \leq 1/\sqrt{3}$, the natural flow speed of information in the QGP phase. There is a longitudinal velocity which is needed to describe rapidity spectra, and there is a hadronization surface motion, aside of many further parameters one may wish to use to model profile of velocity of flowing matter.

The resulting yields of final state hadronic particles are most conveniently characterized taking the Laplace transform of the accessible phase space. This approach generates a function which, in its mathematical properties, is identical to the partition function. For example, for the open strangeness sector, we find (with no flow),

$$\mathcal{L}\left[e^{-E_i/T_{\rm f}} \prod_{k\in i} \gamma_k \lambda_k\right] \propto \ln \mathcal{Z}_{\rm s}^{\rm HG}\,. \tag{11}$$

It is important to keep in mind that:

a. Eq. (11) does not require formation of a phase comprising a gas of hadrons, but is not inconsistent with such a step in evolution of the matter; Eq. (11) describes not a partition function, but just a look-alike object arising from the Laplace transform of the accessible phase space;

b. the final particle abundances measured in an experiment are obtained after all unstable hadronic resonances 'j' are allowed to disintegrate, contributing to the yields of stable hadrons;

c. in some experimental data, it is important to distinguish the two light quark flavors, for example experiments are only sensitive to Ξ^- and not Ξ^0 and an average over isospin does not occur.

The unnormalized particle multiplicities arising are obtained differentiating Eq. (11) with respect to particle fugacity. The relative particle yields are simply given by ratios of corresponding chemical factors, weighted with the size of the momentum phase space accepted by the experiment. The ratios of strange antibaryons to strange baryons *of same particle type* are, in our approach, simple functions of the quark fugacities.

4.3. Strange hadrons at SPS

We expect in sudden hadronization chemical non-equilibrium at hadron freeze-out. For strangeness, $\gamma_{\rm s} \neq 1$, has been seen early on in experimental data, [29]. Full chemical non-equilibrium has been first noted in the study of the S–Au/W/Pb collisions at 200A GeV [30]. Fitting the yields of hadrons observed, it has been reported that the statistical significance increased when chemical non equilibrium was introduced. The statistical significance is derived from the statistical error:

$$\chi^2 \equiv \frac{\sum_j (R^j_{\rm th} - R^j_{\rm exp})^2}{(\Delta R^j_{\rm exp})^2}\,. \tag{12}$$

It is common to normalize the total error χ^2 by the difference between the number of data points and parameters used, the so called 'dof' (degrees of freedom) quantity. For systems we study, with a few degrees of freedom (typically 5–15), a statistically significant fit requires that $\chi^2/{\rm dof} < 1$. For just a few 'dof', the error should be as small as $\chi^2/{\rm dof} < 0.5$. The usual requirement $\chi^2 \to 1$ is only applying for infinitely large 'dof'.

Turning to the Pb–Pb system at 158A GeV collision energy, we consider particle listed in table 1, top section from the experiment WA97, for $p_\perp > 0.7\,{\rm GeV}$, within a narrow $\Delta y = 0.5$ central rapidity window. Further below are shown results from the large acceptance experiment NA49, extrapolated by the collaboration to full 4π phase space coverage. The total error χ^2 for the two result columns is shown at the bottom of this table along with the number of data points 'N', parameters 'p' used, and number of (algebraic) redundancies 'r' connecting the experimental results. For $r \neq 0$, it is more appropriate to quote the total χ^2, since the statistical relevance condition is more difficult to establish given the constraints, but since $\chi^2/(N-p-r) < 0.5$, we are certain to have a valid description of hadron multiplicities. We will return to discuss the yields of $\Omega, \overline{\Omega}$ at the end of this subsection.

In second last column, the superscript 's' means that $\lambda_{\rm s}$ is fixed by strangeness balance and, superscript '$\gamma_{\rm q}$', in two last columns, means that $\gamma_{\rm q} = \gamma_{\rm q}^{\rm c} = e^{m_\pi/2T_{\rm f}}$, is fixed to maximize the entropy content in the hadronic phase space. The fits presented are obtained with latest NA49 experimental results, i.e., have updated ${\rm h}^-/b$, newly published ϕ yield [32], and we predict the $\bar{\Lambda}/\bar{\rm p}$ ratio. b is here the number of baryon participants, and ${\rm h}^- = \pi^- + {\rm K}^- + \bar{\rm p}$ is the yield of stable negative hadrons which includes pions, kaons and antiprotons. We see, comparing the two columns, that strangeness conservation (enforced in second last column) is consistent with the experimental data shown, enforcing it does not change much the results for particle multiplicities.

Table 1
WA97 (top) and NA49 (bottom) Pb–Pb 158A GeV collision hadron ratios compared with phase space fits.

Ratios	Ref.	Exp. Data	$\mathrm{Pb}\vert^{\mathrm{s},\gamma_\mathrm{q}}$	$\mathrm{Pb}\vert^{\gamma_\mathrm{q}}$
Ξ/Λ	[33]	0.099 ± 0.008	0.096	0.095
$\overline{\Xi}/\bar{\Lambda}$	[33]	0.203 ± 0.024	0.197	0.199
$\bar{\Lambda}/\Lambda$	[33]	0.124 ± 0.013	0.123	0.122
$\overline{\Xi}/\Xi$	[33]	0.255 ± 0.025	0.251	0.255
$\mathrm{K}^+/\mathrm{K}^-$	[34]	1.80± 0.10	1.746	1.771
K^-/π^-	[35]	0.082±0.012	0.082	0.080
$\mathrm{K}^0_\mathrm{s}/b$	[36]	0.183 ± 0.027	0.192	0.195
h^-/b	[32]	1.97 ± 0.1	1.786	1.818
ϕ/K^-	[37]	0.145 ± 0.024	0.164	0.163
$\bar{\Lambda}/\bar{\mathrm{p}}$	$y=0$		0.565	0.568
$\bar{\mathrm{p}}/\pi^-$	all y		0.017	0.016
	χ^2		1.6	1.15
	$N;p;r$		9;4;1	9;5;1

The six parameters $(T, v_\mathrm{c}, \lambda_\mathrm{q}, \lambda_\mathrm{s}, \gamma_\mathrm{q}, \gamma_\mathrm{s})$ describing the particle abundances are shown in the top section of table 2. Since the results of the WA97 experiment are not covering the full phase space, there is a reasonably precise value found for one velocity parameter, taken to be the spherical surface flow velocity v_c of the fireball hadron source.

As in S-induced reactions where $\lambda_\mathrm{s} = 1$ [30], now in Pb-induced reactions, a value $\lambda_\mathrm{s}^\mathrm{Pb} \simeq 1.1$ characteristic for a source of freely movable strange quarks with balancing strangeness in presence of strong Coulomb potential [31, page 3568], i.e., with $\tilde{\lambda}_\mathrm{s} = 1$, is obtained. Since all chemical non equilibrium studies of the Pb–Pb system converge to the case of maximum entropy, we have presented the results with fixed $\gamma_\mathrm{q} = \gamma_\mathrm{q}^\mathrm{c} = e^{m_\pi/2T_\mathrm{f}}$. The large values of $\gamma_\mathrm{q} > 1$, seen in table 2, confirm the need to hadronize the excess entropy of the QGP possibly formed. This value is derived from both the specific negative hadron h^-/b abundance and from the relative strange hadron yields.

The fits shown in table 2 satisfy comfortably the constraint that $E/S > T$ discussed in subsection 4.1. One of the interesting quantitative results of this analysis is shown in the bottom section of table 2: the yield of strangeness per baryon, $s/b \simeq 0.7$. We see, in lower portion of table 2, that near strangeness balance is obtained as result of the fit.

The most rarely produced hadron is the triply strange $\Omega(\mathrm{sss})$ and $\overline{\Omega}(\overline{\mathrm{sss}})$ which are the heaviest stable hadrons, $M_\Omega = 1672\,\mathrm{MeV}$. The phase space for $\overline{\Omega}$ is ten times smaller than that for $\overline{\Xi}$ at the conditions of chemical freeze-out we have obtained, and any non-statistical hadronization contribution would be first visible in the Ω and $\overline{\Omega}$ production pattern. For the parameters as in table 2, the $\overline{\Omega}$ yields reported by the experiment WA97 are under predicted by nearly factor two. This yield excess originates at lowest $m_\perp$. The 'failure' of a statistical hadronization model to describe $\overline{\Omega}$ (and by 30% Ω) yields has several possible explanations.

Table 2
Upper section: statistical model parameters which best describe the experimental results for Pb–Pb data seen in Fig. 1. Bottom section: energy per entropy, antistrangeness, net strangeness of the full hadron phase space characterized by these statistical parameters. In column two, we fix λ_s by requirement of strangeness conservation, and in this and next column we fix $\gamma_q = \gamma_q^c$. Superscript * indicates values which are result of a constraint.

	$\mathrm{Pb}\vert_v^{s,\gamma_q}$	$\mathrm{Pb}\vert_v^{\gamma_q}$
T [MeV]	151 ± 3	147.7 ± 5.6
v_c	0.55 ± 0.05	0.52 ± 0.29
λ_q	1.617 ± 0.028	1.624 ± 0.029
λ_s	1.10*	1.094 ± 0.02
γ_q	$\gamma_q^{c*} = e^{m_\pi/2T_f}$=1.6	$\gamma_q^{c*} = e^{m_\pi/2T_f}$=1.6
γ_s/γ_q	1.00 ± 0.06	1.00 ± 0.06
E/b[GeV]	4.0	4.1
s/b	0.70 ± 0.05	0.71 ± 0.05
E/S[MeV]	163 ± 1	160 ± 1
$(\bar{s}-s)/b$	0*	0.04 ± 0.05

Ω and $\overline{\Omega}$ enhancement could be caused by strangeness pre-clustering in the deconfined phase [8]. This would enhance all multistrange hadrons, but most prominently the phase space suppressed Ω and $\overline{\Omega}$ yields. This mechanism would work only if pairing of strange quarks would be significant near to phase transition. There is the possibility that distillation of strangeness followed by break up of strangelets which process could contribute to Ω and $\overline{\Omega}$ production. The decay of disoriented chiral condensates has also been considered, [38].

In view of these pre and post-dictions of the Ω and $\overline{\Omega}$ anomalous yield, one should abstain from introducing these particles into statistical hadronization model fits. We note that the early statistical descriptions of Ω and $\overline{\Omega}$ yields have not been sensitive to the problems we described [24,39]. In fact, as long as the parameter γ_q is not considered, it is not possible to describe the experimental data at the level of precision that would allow recognition of the Ω and $\overline{\Omega}$ excess yield within statistical hadronization. For example, a chemical equilibrium fit, which includes the Ω and $\overline{\Omega}$ yield has for 18 fitted data points with two parameters a $\chi^2/\mathrm{dof} = 37.8/16$ [40]. Such a fit is quite unlikely to contain all the physics even if its appearance to untrained eye is suggesting a very good description of experimental data.

4.4. Strangeness at RHIC

In the likely event that the QGP formed at RHIC evolves towards strangeness chemical equilibrium abundance, or possibly even exceeds it, we should expect a noticeable over occupancy of strangeness as measured in terms of chemical equilibrium final state hadron abundance. Because much of the strangeness is in the baryonic degrees of freedom, the kaon to pion ratio should appear suppressed, compared to SPS results. A more penetrating effect of the hadronization of strangeness rich QGP at RHIC is the formation of strange

baryons and antibaryons. This high phase space occupancy is one of the requirements for the enhancement of multistrange (anti)baryon production, which is an important hadronic signal of QGP phenomena [2,4,8,5]. In particular, we hope that hadrons produced in phase space with a small probability, such as Ω, $\overline{\Omega}$, will be observed with a yield above these expectations, continuing the trend seen at SPS.

Many results from RHIC $\sqrt{s_{\rm NN}} = 130$ GeV run are still preliminary and the following quantitative discussion is probably not the final word in this matter. However, the results we find are very interesting, and in qualitative agreement with the sudden QGP break up reaction picture. The data are mainly obtained at the central rapidity region where, due to approximate longitudinal scaling, the effects of flow cancel and we can evaluate the full phase space yields in order to obtain particle ratios. We do not explore trivial results such as $\pi^+/\pi^- = 1$, since the large hadron yield combined with the flow of baryon isospin asymmetry towards the fragmentation rapidity region assures us that this result will occur to a great precision. We also do not use the results for $\rm K^*, \bar{K}^*$ since these yields depend on the degree of rescattering of resonance decay products [41,12]. The data we use has been reported in conference reports of the STAR collaboration of Summer 2001, which as available are combined with data of PHENIX, BRAHMS, PHOBOS, for more discussion of the data origin, see [42]. We assume, in our fit in table 3, that the multistrange weak interaction cascading $\Xi \to \Lambda$, in the STAR result we consider, is cut by vertex discrimination and thus we use these yields without weak interaction corrections.

We first look at the last column in table 3, the chemical equilibrium fit. Its large χ^2 originates in the inability to account for multistrange $\overline{\Xi}$, Ξ. Similar results are presented in Ref.[42], in an equilibrium fit which does not include multistrange hadrons. The equilibrium fit yields $E/S = 159\,{\rm MeV} < T = 183$ MeV contradicting the conditions we discussed in depth in subsection 4.1. On the other hand, the chemical nonequilibrium fits come out to be in perfect agreement with data, and are consistent with the QGP hadronization picture since $E/S = 163 > T = 158$ MeV and $\gamma_{\rm s}, \gamma_{\rm q} > 1$. The value of the hadronization temperature $T = 158$ MeV is below the central expected equilibrium phase transition temperature, this hadronization temperatures at RHIC is consistent with sudden breakup of a supercooled QGP fireball. The inclusion of the yields of multistrange antibaryons in the RHIC data analysis, along with chemical non-equilibrium, allows to discriminate the different reaction scenarios.

We look next at the strangeness content, $s/b = 6$, in table 3: the full QGP phase space would have yielded 8.6 strange quark pairs per baryon at $\lambda_{\rm q} = 1.085$, as we will show below in Fig. 5. Thus we conclude that $\gamma_{\rm s}^{\rm QGP} = 6/8.6 = 0.7$. With this value, and using the fitted value $\gamma_{\rm s}^{\rm HG} = 2.1$, we compute $\gamma_{\rm s}^{\rm HG}/\gamma_{\rm s}^{\rm QGP} = 2.1/0.7 = 3$. The fact that the strangeness phase space in QGP is not fully saturated is, on a second careful look, in qualitative agreement with kinetic theory predictions, adjusting for the observed RHIC-130 run conditions.

The value of the thermal energy content, $E/b = 25$ GeV, seen in table 3 is also in very good agreement with expectations once we allow for the kinetic energy content, associated with longitudinal and transverse motion. The energy of each particle is 'boosted' with the factor $\gamma_\perp^v \cosh y_\parallel$. For $v_\perp = c/\sqrt{3}$, we have $\gamma_\perp^v = 1.22$. The longitudinal flow range is about ± 2.3 rapidity units, according to PHOBOS results. To obtain the the energy increase due to longitudinal flow, we have to multiply by the average, $\int dy_\parallel \cosh y_\parallel / y_\parallel \to$

Table 3
Fits of central rapidity hadron ratios for RHIC $\sqrt{s_{\rm NN}} = 130$ GeV run. Top section: experimental results, followed by chemical parameters, physical property of the phase space, and the fit error. Columns: data, full non-equilibrium fit, nonequilibrium fit constrained by strangeness conservation and supersaturation of pion phase space, and in the last column, equilibrium fit constrained by strangeness conservation, upper index * indicates quantities fixed by these considerations.

	Data	Fit	Fit $\mathrm{s}-\bar{\mathrm{s}}=0$	$\mathrm{Fit}^{\mathrm{eq}}$ $\mathrm{s}-\bar{\mathrm{s}}=0$
$\bar{\mathrm{p}}/\mathrm{p}$	0.64 ±0.07	0.637	0.640	0.587
$\bar{\mathrm{p}}/\mathrm{h}^-$		0.068	0.068	0.075
$\overline{\Lambda}/\Lambda$	0.77 ±0.07	0.719	0.718	0.679
Λ/h^-	0.059±0.001	0.059	0.059	0.059
$\overline{\Lambda}/\mathrm{h}^-$	0.042±0.001	0.042	0.042	0.040
$\overline{\Xi}/\Xi$	0.83 ±0.08	0.817	0.813	0.790
Ξ^-/Λ	0.195±0.015	0.176	0.176	0.130
$\overline{\Xi^-}/\overline{\Lambda}$	0.210±0.015	0.200	0.200	0.152
$\mathrm{K}^-/\mathrm{K}^+$	0.88 ±0.05	0.896	0.900	0.891
K^-/π^-	0.149±0.020	0.152	0.152	0.145
$\mathrm{K_S}/\mathrm{h}^-$	0.130±0.001	0.130	0.130	0.124
Ω/Ξ^-		0.222	0.223	0.208
$\overline{\Omega}/\overline{\Xi^-}$		0.257	0.256	0.247
$\overline{\Omega}/\Omega$		0.943	0.934	0.935
T		158± 1	158± 1	183± 1
γ_{q}		1.55±0.01	1.58±0.08	1^*
λ_{q}		1.082±0.010	1.081±0.006	1.097±0.006
γ_{s}		2.09±0.03	2.1±0.1	1^*
λ_{s}		1.0097±0.015	1.0114^*	1.011^*
E/b[GeV]		24.6	24.7	21
s/b		6.1	6.2	4.2
S/b		151	152	131
E/S[MeV]		163	163	159
χ^2/dof		2.95/(10−5)	2.96/(10−4)	73/(10−2)

$\sinh(2.3)/2.3 = 2.15$, for a total average increase in energy by factor 2.62, which takes the full energy content to $E^v/b \simeq 65$ GeV as expected.

We now consider what experimental hadron yield results imply about total strangeness yield in the RHIC fireball. First, we sum up the yield of strange quarks contained in hyperons. We have in singly strange hyperons 1.5 times the yield observed in Λ, since $\Sigma^{\pm}$ remain unobserved. Also, accounting for the doubly strange Ξ^- which are half of the all Ξ, and contain two strange quarks, we have:

$$\frac{\langle s\rangle_{\mathrm{Y}}}{\mathrm{h}^-} = 1.5\cdot 0.059 + 2\cdot 2\cdot 0.195\cdot 0.059 = 0.133\,.$$

Allowing for the unobserved Ω at the theoretical rate, this number increases to $\langle s\rangle_{\rm Y}/{\rm h}^- = 0.14$. Repeating the same argument for antihyperons the result is 0.10. s and $\bar{\rm s}$ content in kaons is four times that in $\rm K_S$ and thus the total strangeness yield is

$$\frac{\langle {\rm s}+\bar{\rm s}\rangle}{{\rm h}^-} = 0.76\,,$$

with 32% of this yield contained in hyperons and antihyperons. Up to this point, the analysis is based on direct measurements and established particle yields.

We now estimate the increase in the 'strangeness suppression' factor $W_{\rm s}$, Eq. (6). Correcting for presence of $\rm K^-$ among negatively charged hadrons, and assuming that all three pions are equally abundant, we find:

$$\frac{\langle {\rm s}+\bar{\rm s}\rangle}{\pi^- + \pi^+ + \pi^0} \simeq 0.30\,.$$

The total number of pions produced comprises pions arising from resonance decays and from projectile and target fragments. Thus, as little as half of the pions are originating in the newly made $\rm q\bar{q}$ pairs. In the RHIC $\sqrt{s_{\rm NN}} = 130$ GeV run, $W_{\rm s} \simeq 0.6$. The increase compared to SPS is largely due to strangeness content in hyperons. Considering that $\gamma_{\rm s}^{\rm QGP} \simeq 0.7$ at $\sqrt{s_{\rm NN}} = 130$ GeV, there is still space for a further strangeness yield rise at highest RHIC energy, and we hope and expect $W_{\rm s} \to 1$ when initial temperatures rises to well above strange quark mass for sufficient length of time.

4.5. Strangeness as signature of deconfinement

The rate of strangeness production in QGP is sensitive to the temperature achieved at the time gluons reach chemical and thermal equilibrium. There is considerable uncertainty how short the time required to relax strangeness flavor in the thermal gluon medium is. Consideration of a small strangeness mass found in lattice studies of strange hadrons implies rapid strangeness chemical equilibration. There is also the probable acceleration of equilibration due to the next to leading order effects (K-factor). In view of this, we now discuss a benchmark yield of strangeness, assuming that the equilibration process leads to near chemical equilibrium conditions for hadronizing QGP. Specifically, the light quark abundance in the quark–gluon plasma phase is considered at the equilibrium yield, while the strange quark yield is characterized by the QGP-phase space occupancy before hadronization, $\gamma_{\rm s}^{\rm QGP}$.

We consider the ratio of equilibrium strangeness density, arising in the Boltzmann gas limit, to the baryon density in a QGP fireball yields:

$$\frac{\rho_{\rm s}}{\rho_{\rm b}} = \frac{s}{b} = \frac{\gamma_{\rm s}^{\rm QGP}\frac{3}{\pi^2}T^3(m_{\rm s}/T)^2K_2(m_{\rm s}/T)}{\frac{2}{3}\left(\mu_{\rm q}T^2+\mu_{\rm q}^3/\pi^2\right)}\,. \tag{13}$$

To first approximation, perturbative thermal QCD corrections cancel in the ratio. For $m_{\rm s} = 200$ MeV and $T = 150$ MeV, we have:

$$\frac{s}{b} \simeq \gamma_{\rm s}^{\rm QGP}\frac{0.7}{\ln\lambda_{\rm q} + (\ln\lambda_{\rm q})^3/\pi^2}\,. \tag{14}$$

The relative yield s/b is in the approximation considered, nearly temperature independent, which allows to gain considerable understanding of strangeness production. This

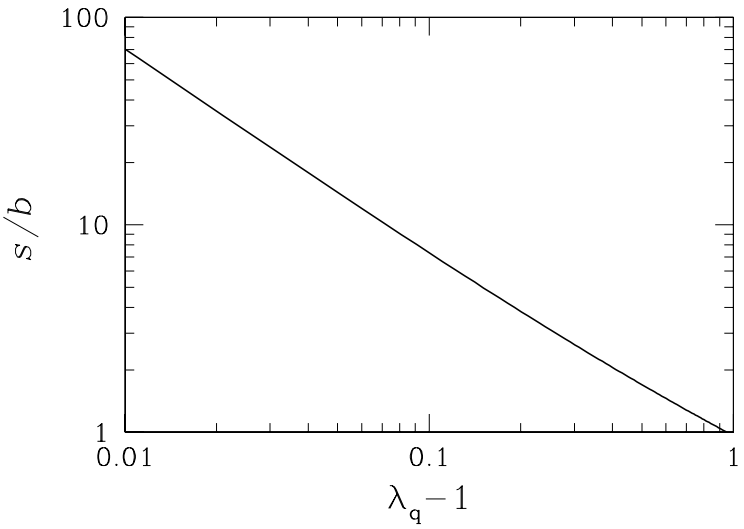

Figure 5. Strangeness yield per baryon as function of λ_q in equilibrated quark-gluon plasma.

ratio is mainly dependent on the value of λ_q. This light quark fugacity pertinent to the final state hadrons is usually quite well determined and does not vary depending on the strategy of data analysis. In the sudden hadronization model, the value in QGP is imprinted on the yields of final state hadrons.

We show in Fig. 5, as function of $\lambda_q - 1$ (variable chosen to enlarge the interesting region $\lambda_q \to 1$), the expected relative yield per baryon originating in the QGP, defined in Eq. (14) with $\gamma_s^{QGP} = 1$. At top SPS energy, we see that the equilibrium yield is at 1.5 strange pairs per participating baryon (for $\lambda_q \simeq 1.5$–1.6). In p–p collisions at the corresponding energy, the yield is below 0.3 strange pair per participant [23]. We note that the p–p reaction yield is suppressed by factor 2 compared to the canonical yield resulting when one attempts to use statistical canonical description to size up the phase space. The actual experimental yield, is 2.5 times the yield in p–p reactions, see table 2, this is however only half as large as in an equilibrated QGP, see Fig. 5. There is need to have $\gamma_s^{QGP} \simeq 0.5$–$0.7$, in both p–p reaction and the SPS top energy Pb–Pb reactions. The explanation of this is that the QGP system did not get to be hot enough for long enough time to fill the small p–p and very large Pb–Pb phase spaces.

At the RHIC 130 GeV run, the value $\lambda_q = 1.09$ allows to understand many particle yields at central rapidity. We see, in Fig. 5, that specific strangeness yield in a QGP fireball at equilibrium is expected to be an order of magnitude greater than currently observed at SPS top energy. However, comparing to general hadron multiplicity, only a factor 1.5–2 further strangeness enhancement can at most be expected at RHIC, the remarkable feature of the RHIC situation is that this enhancement is found in the (multistrange) baryon abundance. Specially, given the large strangeness per baryon ratio, Fig. 5, baryons and antibaryons produced at RHIC are mostly strange [22]. We are not aware of any reaction model other than QGP formation and hadronization which could produce this type of anomaly.

While the specific strangeness yield s/b is a clear indicator for the extreme conditions reached in heavy ion collisions, perhaps an equally interesting observable is the occu-

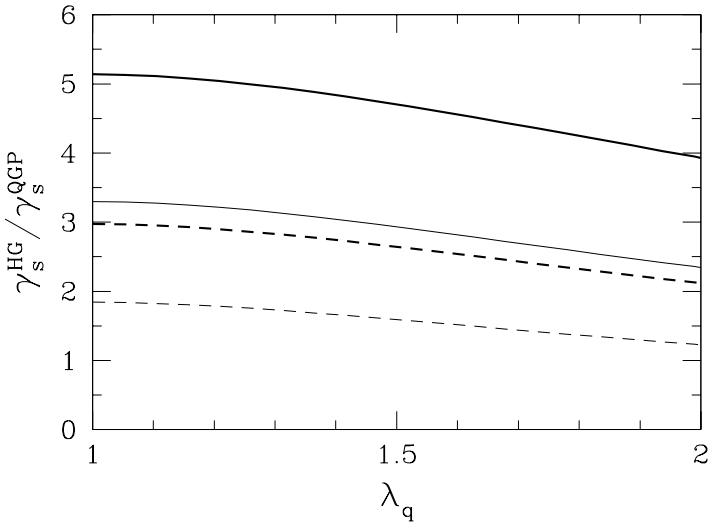

Figure 6. Strangeness occupancy γ_s ratio HG/QGP in sudden hadronization as function of λ_q. Solid lines $\gamma_q = 1$, and short dashed $\gamma_q = 1.6$. Thin lines for $T = 170$ and thick lines $T = 150$ MeV, common to both phases.

pancy of the hadron strangeness phase space, γ_s^{HG}. The interesting result to expect is an enhancement due to the need to hadronize, into a strangeness poor phase, the QGP strangeness excess. To see this, we compare the phase space of strangeness in QGP with that of resulting HG. The absolute yields must be the same in both phases. This hadronization condition allows to relate the two phase space occupancies in HG and QGP, by equating the strangeness content in both phases. Canceling the common normalization factor $T^3/(2\pi^2)$, we obtain:

$$\gamma_s^{QGP} V^{QGP} g_s \left(\frac{m_s}{T^{QGP}}\right)^2 K_2\left(\frac{m_s}{T^{QGP}}\right) \simeq \gamma_s^{HG} V^{HG} \left[\frac{\gamma_q \lambda_q}{\lambda_s} F_K + \frac{\gamma_q^2}{\lambda_q^2 \lambda_s} F_Y\right], \tag{15}$$

where F_K and F_Y are the phase spaces of kaons and hyperons, respectively. We have, without loss of generality, followed the $\bar{s}$ carrying hadrons in the HG phase space, and we have, in first approximation, omitted the contribution of multistrange antibaryons. We now use the condition that strangeness is conserved to eliminate λ_s, in Eq. (15), and obtain,

$$\frac{\gamma_s^{HG}}{\gamma_s^{QGP}} \frac{V^{HG}}{V^{QGP}} = \frac{g_s W(m_s/T^{QGP})}{\sqrt{(\gamma_q F_K + \gamma_q^2 \lambda_q^{-3} F_Y)(\gamma_q F_K + \gamma_q^2 \lambda_q^3 F_Y)}}\,. \tag{16}$$

In sudden hadronization, $V^{HG}/V^{QGP} \simeq 1$, the growth of volume is negligible, $T^{QGP} \simeq T^{HG}$, the temperature is maintained across the hadronization front, and the chemical occupancy factors in both states of matter accommodate the different magnitude of the particle phase space. In this case, the QGP strangeness when 'squeezed' into the smaller HG phase space results in $\gamma_s^{HG}/\gamma_s^{QGP} > 1$. We show, in Fig. 6, the enhancement of phase space occupancy expected in sudden hadronization of the QGP. The temperature range $T = 150$ MeV (thick lines) and $T = 170$ MeV (thin lines) spans the range considered

today at SPS and RHIC. The value of γ_q is in range of the chemical equilibrium in HG, $\gamma_q = 1$ (solid lines), to the expected excess in sudden hadronization, $\gamma_q = 1.6$ (short dashed lines).

We note that, for the top SPS energy range where $\lambda_q = 1.5$–1.6, sudden hadronization analysis of data implies $T \simeq 150\,\mathrm{MeV}$, $\gamma_q \simeq 1.6$, and the value of γ_s increases across hadronization by factor 2.7 . Since the yield of strangeness seen at SPS implies $\gamma_s^{QGP} \simeq 0.6$, this in turn implies $\gamma_s^{HG} \simeq 1.6 \simeq \gamma_q^{HG}$, as is indeed found in hadron production analysis in the sudden hadronization picture, table 2. Because accidentally $\gamma_s^{HG}/\gamma_q^{HG} \simeq 1$, one can also model the hadronization at SPS energy in terms of an equilibrium hadronization model. The pion enhancement associated with the high entropy phase can be accommodated by use of two temperatures, one for the determination of absolute particle yields, and another for determination of the spectral shape. Such an approach has similar number of parameters, and comparable predictive power.

However, the SPS condition, $\gamma_s^{HG}/\gamma_q^{HG} \simeq 1$, is not present at the RHIC energy range, where the hadron phase space occupancy for strangeness is significantly larger than for light quarks, see table 3. QGP hadronization dynamics should emerge clearly from the study of (multi)strange hadron yields at RHIC. Using the yields of (multi) strange baryons and antibaryons it is possible to discriminate against trivial equilibrium hadronic gas models. Moreover, at RHIC we find a very strong strange baryon and antibaryon yield which is not accessible in kinetic parton models.

5. FINAL REMARKS

The deconfined thermal phase manifests itself through its gluon content, which generates in thermal collision processes a clear strangeness fingerprint of QGP. The SPS strangeness results decisively show interesting new physics, with a significant excess of strangeness and strange antibaryons, and spectral symmetry between baryons and antibaryons. We see, at SPS and at RHIC, considerable convergence of the hadron production around properties of suddenly hadronizing entropy and strangeness rich QGP. We see hadronization into pions, at $\gamma_q \to \gamma_q^c = e^{m_\pi/2T_f} \simeq 1.6$, which is an effective way to convert excess of entropy in the plasma into hadrons. Because of large value of γ_q the strange particle signature of QGP hadronization become more extreme and clear at RHIC, as the strangeness excess is covered by the general hadron yield excess at SPS. The systematic behavior as function of collision energy, and other collision system parameters, will in future provide a cross check of our reaction picture.

We have not advocated that the understanding of QGP can or should be based on a comparison of the A–A collision system with the elementary systems such as p–p or even e^+–e^-. We simply do not know at this time if elementary interaction system is in any fundamental way different. It could well be that once there is enough energy deposition, the relativistic Maxwell demon which leads to the formation of the statistical high entropy QCD state is operating in both the small and the big system, and that the difference in the observables arises due to a change in the internal excitation (temperature), and size (and thus lifespan). For example, there would be no outward (transverse) flow of matter and little strangeness thermal production expected in p–p system, compared to A–A collision system. The smaller phase space of the p–p system is easier to equilibrate than the A–A

collision system, leading to further confusion.

It is important to remember that, not only at RHIC, and in near future at LHC, QGP can be studied. It is very probable that the onset of deconfinement occurs at quite modest energies, perhaps in collisions of 20–40A GeV Pb projectiles with a laboratory target. An alternate method of QGP exploration is the study of the energy domain near the transition. Formation of QGP phase is an endothermic process with onset of entropy and strangeness production, and in experiments near to the condition for phase transformation, one should be able to recognize these properties quite clearly: for example, by the onset as function of energy and of reaction volume of multistrange antibaryon production. The measurement of yields as function of energy, and volume (excitation functions) should provide information about the nature of the transition to this new phase of matter.

In closing, we have analyzed available RHIC and high energy SPS results and have demonstrated that these can be easily understood as result of sudden hadronization of a rapidly expanding QGP fireball. We have discussed characteristic nonequilibrium aspects of strangeness yields associated with the QGP fireball explosion. Our analysis shows in detail how and where the hadronic equilibrium models fail to describe the experimental data.

REFERENCES

1. J. Rafelski and R. Hagedorn. From hadron gas to quark matter II. In H. Satz, editor, *Statistical Mechanics of Quarks and Hadrons*, page 253. North Holland, Amsterdam, 1981.
2. J. Rafelski. Extreme states of nuclear matter. In R. Bock and R. Stock, editors, *Workshop on Future Relativistic Heavy Ion Experiment*, page 282. GSI Report 81-6, Darmstadt, 1981.
3. J. Rafelski. Hot hadronic matter. In J. Tran Thanh Van, editor, *New Flavors and Hadron Spectroscopy*, page 619. Editions Frontières, 1981.
4. J. Rafelski, 1982. Extreme states of nuclear matter. *Nucl. Phys.* A, **374**, 489c.
5. J. Rafelski and B. Müller, 1982. Strangeness production in the quark–gluon plasma. *Phys. Rev. Lett.*, **48**, 1066. See: *Phys. Rev. Lett.*, **56**, 2334E (1986).
6. P. Koch, B. Müller, and J. Rafelski, 1986. Strange quarks in relativistic nuclear collisions. *Phys. Rep.*, **142**, 167.
7. P. Koch and J. Rafelski, 1986. Why the hadronic gas description of hadronic reactions works: The example of strange hadrons. *S. Afr. J. Phys.*, **9**, 8.
8. J. Rafelski, 1982. Formation and observables of the quark gluon plasma. *Phys. Rep.*, **88**, 331.
9. J. Rafelski and M. Danos, *Perspectives in High Energy Nuclear Collisions*, NBS-IR 83-2725 Monograph, U.S. Department of Commerce, National Bureau of Standards, June 1983; Updated version appeared in *Nuclear Matter under Extreme Conditions*, D. Heiss, Ed., Springer Lecture Notes in Physics **231**, pp. 362-455 (1985).
10. S.A. Chin, 1978. Transition to hot quark matter in relativistic heavy-ion collision. *Phys. Lett.* B, **78**, 552.
11. S. Hamieh, J. Letessier, and J. Rafelski, 2000. Quark–gluon plasma fireball. *Phys. Rev.* C, **62**, 64901.
12. J. Rafelski, J. Letessier, and G. Torrieri, 2001. Strange hadrons and their resonances: A diagnostic tool of quark–gluon plasma freeze-out dynamics. *Phys. Rev.* C, **64**, 54907.
13. J. Rafelski and J. Letessier, 2000. Sudden hadronization in relativistic nuclear collisions.

Phys. Rev. Lett., **85**, 4695.
14. A. Peshier, B. Kämpfer, and G. Soff, 2000. Equation of state of deconfined matter at finite chemical potential in a quasiparticle description. *Phys. Rev.* C, **61**, 45203.
15. H.A. Weldon, 1982. Covariant calculations at finite temperature: The relativistic plasma. *Phys. Rev.* D, **26**, 1394.
16. H.A. Weldon, 1982. Effective fermion masses of order gT in high temperature gauge theories with exact chiral invariance. *Phys. Rev.* D, **26**, 2789.
17. B. Combridge, 1979. Associated production of heavy flavour states in pp and $\overline{\mathrm{p}}$p interactions: Some QCD estimates. *Nucl. Phys.* B, **151**, 429.
18. J. Letessier, J. Rafelski, and A. Tounsi, 1996. Impact of QCD and QGP properties on strangeness production. *Phys. Lett.* B, **389**, 586.
19. T.S. Biró, E. van Doorn, B. Müller, M.H. Thoma, and X.-N. Wang, 1993. Parton equilibrium in relativistic heavy ion collisions. *Phys. Rev.* D, **48**, 1275.
20. D. Srivastava, M. Mustafa, and B. Müller, 1997. Chemical equilibration of an expanding quark–gluon plasma. *Phys. Lett.* B, **45**, 396.
21. D. Srivastava, M. Mustafa, and B. Müller, 1997. Expanding quark–gluon plasmas: Transverse flow, chemical equilibration and electromagnetic radiation. *Phys. Rev.* C, **56**, 1064.
22. J. Rafelski and J. Letessier, 1999. Expected production of strange baryons and antibaryons in baryon-poor QGP. *Phys. Lett.* B, **469**, 12.
23. A. Wróblewski, 1985. On the strange quark suppression factor in high energy collisions. *Acta Phys. Pol.* B, **16**, 379.
24. F. Becattini, M. Gaździcki, and J. Sollfrank, 1998. On chemical equilibrium in nuclear collisions. *Eur. Phys. J.* C, **5**, 143.
25. P. Koch and J. Rafelski, 1985. Time evolution of strange-particle densities in hot hadronic matter. *Nucl. Phys.* A, **444**, 678.
26. T.S. Biró, 2000. Quark coalescence and hadronic equilibrium. *Hep-ph/0005067*.
27. E. Fermi, 1950. High-energy nuclear events. *Prog. Theo. Phys.*, **5**, 570.
28. E. Fermi, 1953. Multiple production of pions in nucleon–nucleon collisions at cosmotron energies. *Phys. Rev.*, **92**, 452.
29. J. Rafelski, 1991. Strange antibaryons from quark–gluon plasma. *Phys. Lett.* B, **262**, 333.
30. J. Letessier and J. Rafelski, 1999. Chemical non-equilibrium and deconfinement in 200A GeVSulphur induced reactions. *Phys. Rev.* C, **59**, 947.
31. J. Letessier and J. Rafelski, 1999. Diagnostics of QGP with strange hadrons. *Acta Phys. Pol.* B, **30**, 3559.
32. H. Appelshäuser *et al.*, NA49 collaboration, 1999. Baryon stopping and charged particle distributions in central Pb+Pb collisions at 158 GeV per nucleon. *Phys. Rev. Lett.*, **82**, 2471.
33. I. Králik, *et al.*, WA97 collaboration, 1998. Λ, Ξ and Ω production in Pb–Pb collisions at 158A GeV. *Nucl. Phys.* A, **638**, 115.
34. C. Bormann, *et al.*, NA49 collaboration, 1997. Kaon, lambda and antilambda production in Pb+Pb collisions at 158 GeV per nucleon. *J. Phys.* G *Nucl. Part. Phys.*, **23**, 1817.
35. F. Siklér *et al.*, NA49 collaboration, 1999. Hadron production in nuclear collisions from the NA49 experiment at 158A GeV. *Nucl. Phys.* A, **661**, 45c.
36. P.G. Jones *et al.*, NA49 collaboration, 1996. Hadron yields and hadron spectra from the NA49 experiment. *Nucl. Phys.* A, **610**, 188c.
37. S.V. Afanasev *et al.*, NA49 collaboration, 2000. Production of ϕ mesons in p+p, p+Pb and central Pb+Pb collisions at $E_{\mathrm{beam}} = 158A$ GeV. *Phys. Lett.* B, **941**, 59.
38. J. I. Kapusta and S. M. H. Wong, 2001. Is anomalous production of ω and $\overline{\omega}$ evidence for

disoriented chiral condensates? *Phys. Rev. Lett.*, **86**, 4251.
39. J. Letessier, J. Rafelski, and A. Tounsi, 1997. Strangeness in Pb–Pb collisions at 158A GeV. *Phys. Lett.* B, **410**, 315.
40. P. Braun-Munzinger, I. Heppe, and J. Stachel, 1999. Chemical equilibration in Pb+Pb collisions at the SPS. *Phys. Lett.* B, **465**, 15.
41. G. Torrieri and J. Rafelski, 2001. Search for QGP and thermal freeze-out of strange hadrons. *New J. of Phys.*, **3**, 12.
42. P. Braun-Munzinger, D. Magestro, K. Redlich, and J. Stachel, 2001. Hadron production in Au–Au collisions at RHIC. *Phys. Lett.* B, **518**, 41.